



## NOTE

Pathology

# Pathological features of hepatic portal venous gas in a cat

Kazuhiro KOJIMA<sup>1)</sup>, James K. CHAMBERS<sup>1)\*</sup>, Ayano ISHII<sup>2)</sup>, Kazuhito SEGAWA<sup>2)</sup> and Kazuyuki UCHIDA<sup>1)</sup><sup>1)</sup>Laboratory of Veterinary Pathology, Graduate School of Agricultural and Life Sciences, The University of Tokyo, Bunkyo-ku, Tokyo 113-8657, Japan<sup>2)</sup>Sagamihara Animal Medical Centre, Sagamihara, Kanagawa 252-0344, Japan*J. Vet. Med. Sci.*

84(2): 213–217, 2022

doi: 10.1292/jvms.21-0579

Received: 28 October 2021

Accepted: 14 December 2021

Advanced Epub:

27 December 2021

**ABSTRACT.** An 8-year 8-month-old castrated male Munchkin presented with vomiting, anorexia and hypoactivity. Computed tomography revealed excessive gas accumulation within the intestinal lumen and gas bubbles in the liver, spleen, and portal venous system, indicating hepatic portal venous gas. The cat died without any significant improvement, and mild splenomegaly was found at necropsy. Histologically, multiple gas vacuoles were diffusely observed in the liver and spleen. In the stomach, multiple gas vacuoles and scattered focal ulcers were detected within the mucosa. Multifocal hemorrhage was noted in the small and large intestines, whereas gas vacuoles were not present. Based on these findings, a gastric ulcer under high gas pressure may have provided an entry point for gas into the portal venous system.

**KEY WORDS:** feline, hepatic portal venous gas, post mortem

Hepatic portal venous gas (HPVG) is a rare condition that occurs when gas enters the portal venous system. In human medicine, HPVG is associated with necrosis and/or ulceration of the gastrointestinal tract, and is regarded as a poor prognostic sign with a high mortality rate [7]. HPVG has also been reported in dogs and cats with gastrointestinal disease, infection/sepsis, trauma (including iatrogenic trauma), and liver neoplasia [3, 9, 11, 13]. The ingestion of hydrogen peroxide resulted in the development of HPVG in a dog [1]. HPVG is generally diagnosed by radiography, ultrasound, or computed tomography (CT), and the prognosis of canine and feline HPVG cases depends on the underlying diseases [9]. Although the pathogenesis of HPVG remains unclear, it is considered to be caused by increased gas pressure in the intestinal lumen or by alterations in the intestinal mucosa that allow gas to enter the portal venous system through the mesenteric vein [7]. Previous studies on HPVG in animals focused on imaging examinations, and, thus, limited information is currently available on pathological findings. The aim of the present study was to describe the pathological findings of a feline case of HPVG and discuss its pathogenesis.

An 8-year 8-month-old castrated male Munchkin developed vomiting, anorexia, and hypoactivity. While the results of a blood examination were unremarkable, mildly corrugated bowel was noted in the ultrasonographic examination. The cat was treated by administering intravenous omeprazole, metoclopramide, and crystalloid fluid. The next afternoon, the cat vomited and a radiographic examination revealed branching linear gas permeability in the liver and multifocal stippled gas bubbles in the spleen (Fig. 1). The cat collapsed and a CT scan showed excessive gas accumulation within the intestinal lumen as well as gas bubbles in the liver, spleen and portal venous system (Fig. 2). The cat died without any significant improvement, and necropsy was performed on the same day. Mild splenomegaly was detected at necropsy. Multiple vacuoles of approximately 1 to 3 mm in diameter were diffusely observed on the cut surface of the spleen. The heart, lung, stomach, intestines, liver, spleen, kidneys, bladder, and mesenteric and pancreaticoduodenal lymph nodes were collected and fixed in 10% neutral-buffered formalin for a histopathological examination.

Formalin-fixed, paraffin-embedded (FFPE) tissues were sectioned at a thickness of 4 µm and stained with hematoxylin and eosin (HE). Serial sections were subjected to Gram staining and immunohistochemistry. Immunohistochemistry using primary antibodies for von Willebrand factor (vWF) (polyclonal rabbit anti-human vWF; Dako, Tokyo, Japan) and CD31 (polyclonal rabbit anti-human CD31; Novus Biological, Centennial, CO, USA) was performed to identify the vascular endothelium. After heat-induced epitope retrieval with citrate buffer (pH 6.0), sections were incubated with the primary antibodies and then with the Envision polymer (Dako). Sections were visualized with diaminobenzidine tetrahydrochloride and counter-stained with hematoxylin. Oil Red O staining was performed to detect lipid bodies. Formalin-fixed tissue was processed with graded sucrose and placed into

\*Correspondence to: Chambers, J. K.: [achamber@g.ecc.u-tokyo.ac.jp](mailto:achamber@g.ecc.u-tokyo.ac.jp)(Supplementary material: refer to PMC <https://www.ncbi.nlm.nih.gov/pmc/journals/2350/>)

©2022 The Japanese Society of Veterinary Science

This is an open-access article distributed under the terms of the Creative Commons Attribution Non-Commercial No Derivatives (by-nc-nd) License. (CC-BY-NC-ND 4.0: <https://creativecommons.org/licenses/by-nc-nd/4.0/>)

a Tissue-Tek container, which was then filled with Tissue-Tek OCT compound gel (Sakura Finetek, Tokyo, Japan) and frozen in liquid nitrogen. Frozen samples were sectioned at a thickness of 10 µm and stained with Oil Red O.

To detect *Clostridium difficile*, *C. perfringens* and their toxin genes, PCR analyses using specific primer pairs were performed (Supplementary Table 1) [14, 15]. Genomic DNA was extracted from FFPE tissue samples of stomach, small intestine, and large intestine using the QIAamp DNA FFPE Tissue Kit (QIAGEN, Venlo, The Netherlands). PCR was performed using KOD One PCR Master Mix (TOYOBO, Osaka, Japan) by preparing the following reaction mixture: 12.5 µl KOD One PCR Master Mix, 0.75 µl forward primer (10 µM), 0.75 µl reverse primer (10 µM). Template DNA was added between 80 and 100 ng per PCR reaction followed by distilled water to a total volume of 25 µl. Distilled water instead of template DNA was applied for negative controls. The PCR cycle was performed using a 3-step cycling condition according to the manufacturer's instructions as follows: pre-denaturation at 95°C for 3 min followed by 45 cycles of denaturation at 98°C for 10 sec, annealing at temperature corresponding to each primer pair for 5 sec, and extension at 68°C for 5 sec. PCR-amplified products were electrophoresed on 1.5% agarose gels and bands were visualized by UV exposure.

Microscopically, multiple irregular vacuoles (20–100 µm in diameter), which were negative for Oil Red O staining, were observed in the mucosa of the stomach (Fig. 3). These vacuoles were occasionally lined by a flat endothelium that was immunopositive for vWF (Fig. 4) and CD31. Multifocal infiltration of lymphocytes were also scattered in the mucosa, and some of which were accompanied by focal ulcers (Fig. 5). These ulcers were necrotic and poor in granulation tissue, and considered as acute lesions. Gram-positive bacilli were observed on the surface of the ulcers (Fig. 5, Inset). Vessels in the submucosa were

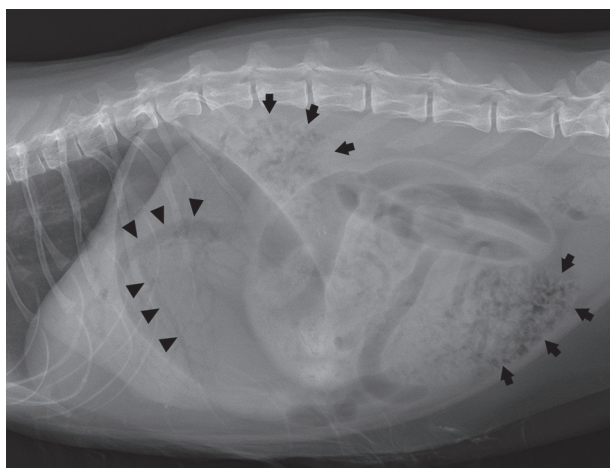


**Fig. 1.** Abdominal radiograph showing branching linear gas permeability in the liver (arrowheads) and multifocal stippled gas bubbles in the spleen (arrows).

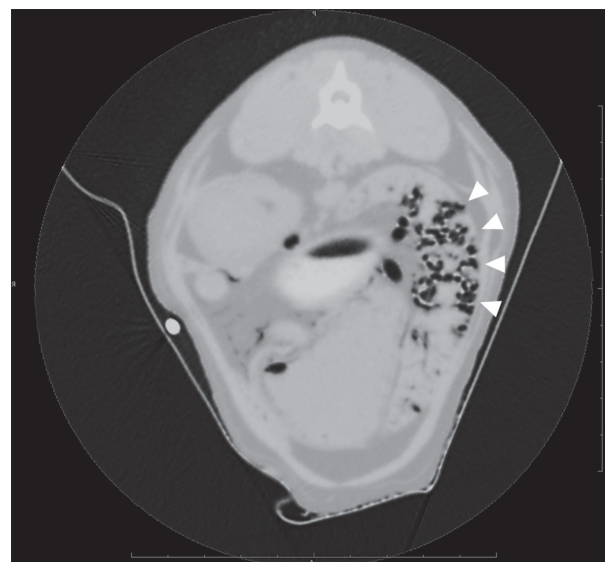


**Fig. 2.** CT image showing multifocal stippled gas bubbles within the spleen (arrowheads).

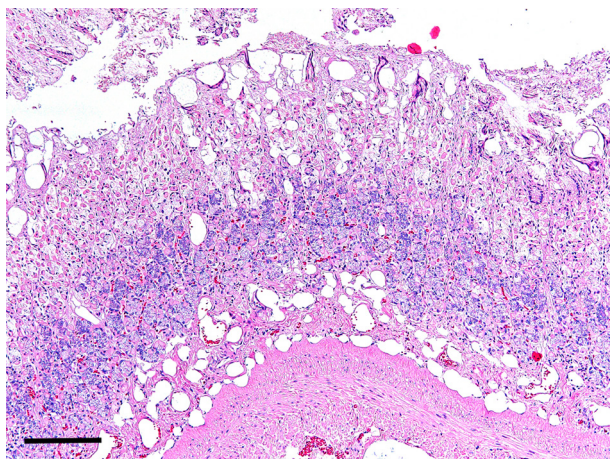


**Fig. 3.** Stomach. Multiple vacuoles in the mucosa. Hematoxylin and eosin. Bar, 200 µm.

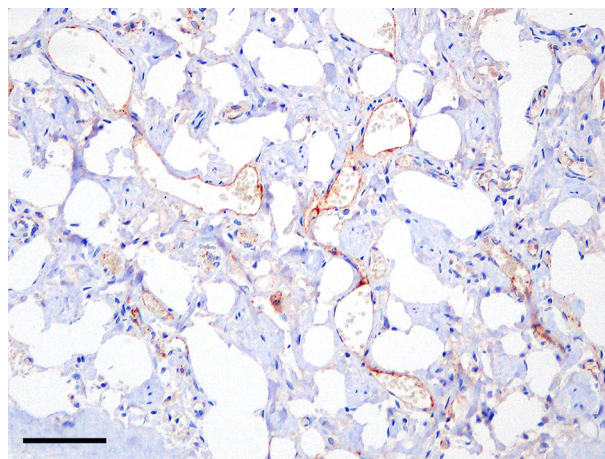


**Fig. 4.** Stomach. Some vacuoles are lined by vWF-positive endothelial cells. Immunohistochemistry. Bar, 50 µm.

irregularly dilated, (Fig. 6) and some of them lacked red blood cells and their endothelial cells were negative for vWF, indicating that there were not only vascular dilation, but also lymphatic dilation. These findings indicated that vacuoles in the mucosa were gas and that some had flowed into the venous and lymphatic vessels.

In the liver, multiple vacuoles (50–700 µm in diameter) were observed from the portal area to the mid-zone of the hepatic lobules (Fig. 7). Vacuoles in the liver were also occasionally lined by an endothelium and immunohistochemistry revealed vascular dilation. These vacuoles were negative for Oil Red O staining. Severe hemorrhage and the mild infiltration of neutrophils and macrophages were noted around the vacuoles. In the spleen, multiple large vacuoles (1–3 mm in diameter) replaced the red pulp. These vacuoles lacked an endothelial lining and were negative for Oil Red O staining. The white pulp was diffusely atrophied. The mild infiltration of neutrophils and macrophages and scattered megakaryocytes were observed in the red pulp. Histologically, bacteria were not observed in the liver and spleen by HE and Gram staining. Based on histological findings, pathological diagnoses were chronic gastritis with acute ulceration and gas embolism in the stomach, liver, and spleen.

In the small and large intestines, multifocal hemorrhage was detected in the lamina propria with the moderate infiltration of lymphocytes and plasmacytes. Gram-negative bacteria were observed on the mucosal surface of the large intestine. The histopathological diagnosis was hemorrhagic enteritis. Chronic bronchitis, marginal emphysema, chronic pancreatitis, unilateral kidney fibrosis, and hemorrhagic lymphadenitis were noted in other organs.

In the PCR analyses, 16S rRNA gene of *C. perfringens* was detected in stomach, small intestine, and large intestine (Fig. 8A), and *cpa* gene (i.e., alpha-toxin gene of *C. perfringens*) in the small and large intestines (Fig. 8B). *Cpb* and *etx* genes (i.e., beta- and epsilon-toxin genes of *C. perfringens*, respectively) were not detected in any tissues examined. 16S rRNA gene of *C. difficile* was

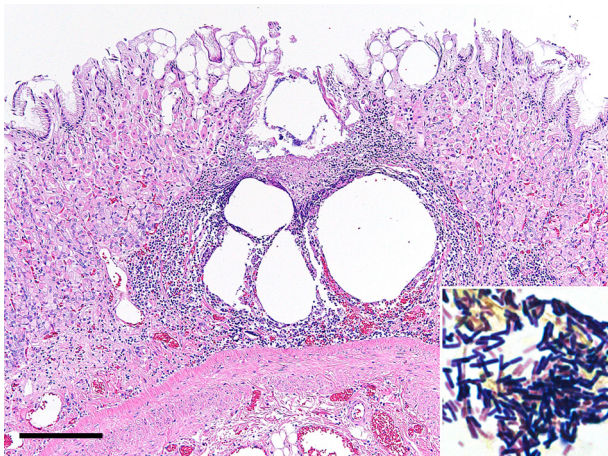


**Fig. 5.** Stomach. A focal ulcer with inflammatory cell infiltration and hemorrhage around vacuoles. Inset: Gram stain. Gram-positive bacilli were observed on the surface of the ulcer. Hematoxylin and eosin. Bar, 200 µm.

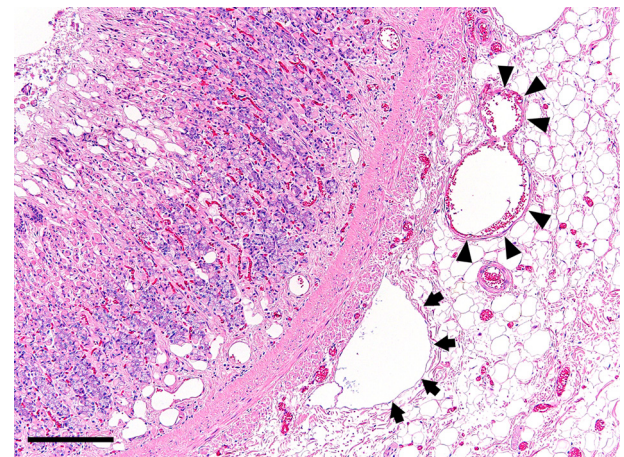


**Fig. 6.** Stomach. Dilated venous (arrowheads) and lymphatic vessels (arrows) surrounded by enriched adipose tissues in the submucosa. Hematoxylin and eosin. Bar, 200 µm.

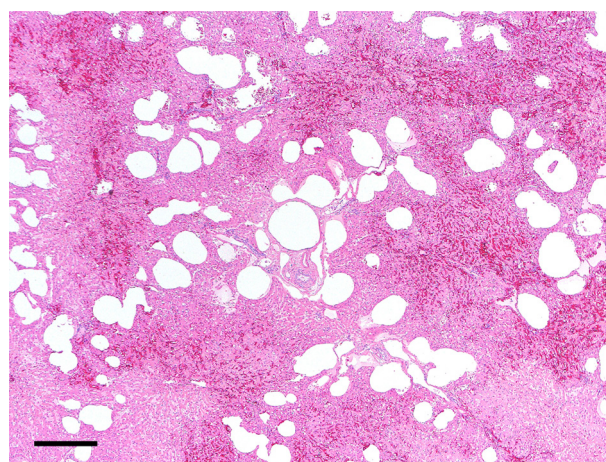


**Fig. 7.** Liver. Gas vacuoles are present in the portal area. Hematoxylin and eosin. Bar, 400 µm.

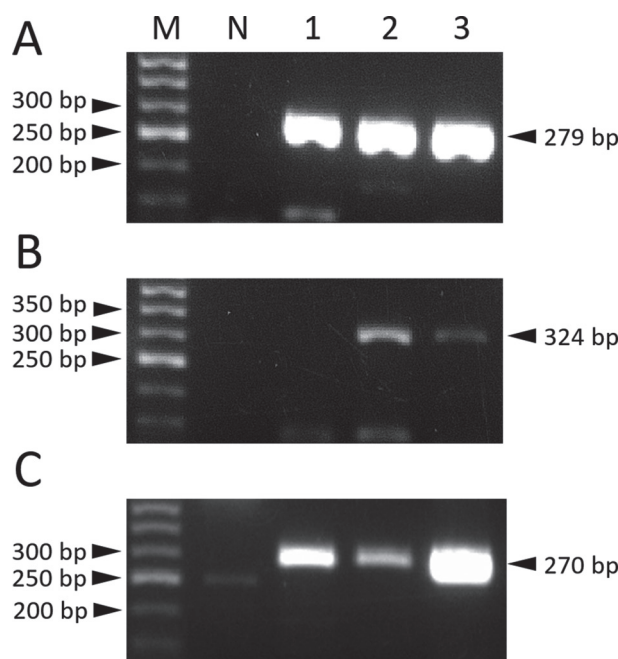


**Fig. 8.** Gel electrophoresis of PCR amplicons for *Clostridium perfringens* 16S rRNA and *cpa* genes, and *C. difficile* 16S rRNA gene. (A) PCR-positive bands for *C. perfringens* 16S rRNA gene in stomach, small intestine and large intestine. (B) PCR-positive bands for *C. perfringens* *cpa* gene in small and large intestines, but not in stomach. (C) PCR-positive bands for *C. difficile* 16S rRNA gene in stomach, small intestine, and large intestine. Abbreviations: bp, base pairs; M, 50 bp ladder; N, negative control; 1, stomach; 2, small intestine; 3, large intestine.

also detected in the stomach, small intestine, and large intestine (Fig. 8C), whereas its toxin genes were not detected.

Although the pathogenesis of HPVG remains unclear, the following three factors are presumed to be involved in human medicine: mucosal injury in the intestines, increased gas pressure, and sepsis caused by gas-producing bacteria [7]. In the present case, a CT examination revealed excessive gas accumulation within the intestinal lumen, indicating an increase in intestinal gas pressure. Histological examinations showed numerous gas vacuoles in the gastric mucosa, and some vacuoles were detected within the blood vessels, indicating that the gastric mucosa was the entry point for gas into the portal venous system. The findings of the present case suggest the involvement of mucosal injury and intestinal pressure in the pathogenesis of HPVG.

In the previous feline case report of HPVG, *C. difficile* toxin was detected from small intestinal contents and considered as a cause of hemorrhagic enteritis and HPVG [13]. In the present case, 16S rRNA and alpha toxin genes of *C. perfringens* were detected in the FFPE tissue samples of small and large intestine, indicating that the cat was infected with *C. perfringens* type A [14]. *C. perfringens* type A is known as a pathogenic bacteria of gas gangrene or foodborne illness in human [2], but its role in feline enteric disease is still unclear because it was detected in both diarrheic and non-diarrheic cats [10]. Nevertheless, *C. perfringens* type A is one of the possible causes of intestinal gas accumulation and hemorrhagic enteritis in this case. The cause of gastric ulcer is still unclear because toxin genes of *C. perfringens* and *C. difficile* was not detected in the stomach possibly due to the small number or absence of pathogenic bacteria in the lesion. However, gastric ulcers occurs under various conditions [12].

HPVG was previously reported in cats and dogs with infection, sepsis, gastrointestinal disease, iatrogenic trauma, trauma, and liver neoplasia [9]. A feline HPVG case with gastric pneumatosis was previously reported [11]; however, the pathological findings of the gastric mucosa associated with HPVG were not described. In the present case, histological findings suggested that the gastric ulcer was the entry point for HPVG. Although hemorrhagic enteritis may be involved in HPVG [11], gas embolism was not observed in the small or large intestines of the present case. Hemorrhagic enteritis and hemorrhage in the lymph nodes may be lesions suggesting sepsis, and, thus, it was not possible to rule out sepsis as the cause of HPVG in the present case.

In human HPVG cases, HPVG may pass into a systemic vein through the liver [6] or a portosystemic shunt [8]. Gas in a systemic vein may cause pulmonary, arterial, or systemic gas embolism [5]. In the present case, gas embolism was noted in the stomach, liver, and spleen. These three organs are connected by the portal venous system: the splenic vein and left gastric vein join the gastrosplenic vein, and the gastrosplenic vein and right gastric vein join the hepatic portal vein [4]. Therefore, HPVG may have flowed back into the spleen via the splenic vein. If gas in the spleen entered via the splenic artery, there may also have been pulmonary or systemic gas embolism; however, this was not detected in the present case. In the stomach of the present case, gas embolism was observed not only in venous vessels, but also in lymphatic vessels. Although lymphatic vessels are also one of the pathways for gas to enter the systemic circulation because the thoracic duct joins the cranial vena cava, gas in the thoracic duct was not detected on CT.

To date, there have only been a few case reports of HPVG in cats. This is the first case report to discuss the pathogenesis of HPVG in a cat based on pathological findings. The findings obtained show that mucosal injury, such as a gastric ulcer, may be an entry point for gas into the portal venous system.

CONFLICT OF INTEREST. The authors declare no potential conflicts of interest with respect to the research, authorship, and/or publication of this manuscript.

## REFERENCES

1. Faverezani, S., Lodi, M. and Pagetti, S. 2009. Imaging diagnosis--portal venous gas in a dog. *Vet. Radiol. Ultrasound* **50**: 312–313. [[Medline](#)] [[CrossRef](#)]
2. Hatheway, C. L. 1990. Toxigenic clostridia. *Clin. Microbiol. Rev.* **3**: 66–98. [[Medline](#)] [[CrossRef](#)]
3. Hutchinson, K. M., Tart, K., Anderson, K. L. and Powell, L. L. 2018. Pneumatosis of the intestines, colon and liver in a young cat. *Vet. Med. Sci.* **4**: 150–158. [[Medline](#)] [[CrossRef](#)]
4. Iuliis, G. D. and Pulerà, D. 2011. The cat. pp. 147–252. In: *The Dissection of Vertebrates*, 2nd ed. (Iuliis, G. D. and Pulerà, D. eds.), Academic Press, Cambridge.
5. Kamikado, C., Nagano, S., Takumi, K., Senokuchi, T., Kubo, M., Mitsue, S., Fukumoto, T., Natugoe, S. and Aikou, T. 2008. Gas embolism caused by portal vein gas: case report and literature review. *Case Rep. Gastroenterol.* **2**: 262–271. [[Medline](#)] [[CrossRef](#)]
6. Kriegshauser, J. S., Reading, C. C., King, B. F. and Welch, T. J. 1990. Combined systemic and portal venous gas: sonographic and CT detection in two cases. *AJR Am. J. Roentgenol.* **154**: 1219–1221. [[Medline](#)] [[CrossRef](#)]
7. Liebman, P. R., Patten, M. T., Manny, J., Benfield, J. R. and Hechtman, H. B. 1978. Hepatic-portal venous gas in adults: etiology, pathophysiology and clinical significance. *Ann. Surg.* **187**: 281–287. [[Medline](#)] [[CrossRef](#)]
8. Mallens, W. M., Schepers-Bok, R., Nicolai, J. J., Jacobs, F. A. and Heyerman, H. G. 1995. Portal and systemic venous gas in a patient with cystic fibrosis: CT findings. *AJR Am. J. Roentgenol.* **165**: 338–339. [[Medline](#)] [[CrossRef](#)]
9. Manfredi, S., Fabbi, M., Bonazzi, M., Leonardi, F., Miduri, F., Parrocchini, I., Daga, E., Gnudi, G. and Volta, A. 2019. Ultrasonographic differentiation between portal venous and parenchymal gas may be important for the prognosis of canine and feline hepatic emphysema: 37 cases. *Vet. Radiol. Ultrasound* **60**: 734–744. [[Medline](#)] [[CrossRef](#)]
10. Silva, R. O. S., Ribeiro, M. G., de Paula, C. L., Pires, I. H., Oliveira Junior, C. A., Diniz, A. N., de Araújo Nunes, T. A. and Lobato, F. C. F. 2020. Isolation of *Clostridium perfringens* and *Clostridioides difficile* in diarrheic and nondiarrheic cats. *Anaerobe* **62**: 102164. [[Medline](#)] [[CrossRef](#)]
11. Spiller, K. T. and Eisenberg, B. W. 2021. Extensive hepatic portal venous gas and gastric pneumatosis in a cat. *Vet. Med. Sci.* **7**: 593–599. [[Medline](#)] [[CrossRef](#)]
12. Sullivan, M. and Yool, D. A. 1998. Gastric disease in the dog and cat. *Vet. J.* **156**: 91–106. [[Medline](#)] [[CrossRef](#)]
13. Walczak, R., Paek, M., Suran, J., Amory, J. T., Specchi, S. and Sanchez, M. 2020. Radiography and ultrasonography of pneumatosis intestinalis in a cat. *Vet. Radiol. Ultrasound* **61**: E26–E30. [[Medline](#)] [[CrossRef](#)]
14. Wu, J., Zhang, W., Xie, B., Wu, M., Tong, X., Kalpoe, J. and Zhang, D. 2009. Detection and toxin typing of *Clostridium perfringens* in formalin-fixed, paraffin-embedded tissue samples by PCR. *J. Clin. Microbiol.* **47**: 807–810. [[Medline](#)] [[CrossRef](#)]
15. Zhang, T., Lin, Q. Y., Fei, J. X., Zhang, Y., Lin, M. Y., Jiang, S. H., Wang, P. and Chen, Y. 2016. *Clostridium difficile* infection worsen outcome of hospitalized patients with inflammatory bowel disease. *Sci. Rep.* **6**: 29791. [[Medline](#)] [[CrossRef](#)]